SSRG International Journal of Recent Engineering Science
ISSN: 2349–7157 / https://doi.org/10.14445/23497157/IJRES-V11I2P102

Volume 11 Issue 2, 9-17, Mar-Apr 2024

Original Article

Adsorption Mechanism of Chlorpyrifos and Dichlorvos Mixture onto Poly-Sorbent Composite Derived from Waste Plastic Products

Sunday O. OLADUNNI[1,2,3], Dauda O. ARAROMI[1,4], Wasiat O. BELLO[1,2,3], Victoria, A. ADEYI[1,2,3], Ilesanmi A. OJO[1,2,5], Abass O. ALADE[1,2,3,4]*

[1]*Department of Chemical Engineering, Ladoke Akintola University of Technology, P.M.B. 4000, Ogbomoso, Nigeria*
[2]*Bioenvironmental, Water, and Engineering Research Group (BWERG), Ladoke Akintola University of Technology, P.M.B. 4000, Ogbomoso, Nigeria*
[3]*LAUTECH SDG 6 Research Cluster (LSDGRC-6), Ladoke Akintola University of Technology, P.M.B. 4000, Ogbomoso, Nigeria*
[4]*Science and Engineering Research Group (SAERG), Ladoke Akintola University of Technology, Ogbomoso, Nigeria*
[5]*Science Laboratory Unit, Al-Hikmah University, Ilorin, Nigeria*

**Corresponding Author : aoalade@lautech.edu.ng*

Received: 14 January 2024 Revised: 23 February 2024 Accepted: 08 March 2024 Published: 27 March 2024

Abstract *- Poly-sorbent Composite was derived from discarded Waste Plastic Chairs (WPC), Waste Polyvinyl Chloride pipes (WPVC), Waste Jerry Cans (WJC) and Waste Electronics Casing (WEC), which were collected at a waste plastic collection center. Each waste plastic was washed, milled to 840 µm and acid-acetylated before being mixed to a composite as Activated Waste Plastic Granule Composite (AWPGC). The functional groups on the AWPGC were determined using Fourier Transform Infrared (FT-IR) Spectroscopy. The composite was used for the removal of the Chlorpyrifos (CPF) and Dichlorvos (DDVP) mixture from the aqueous medium, under the effect of varying time and the data obtained was used to evaluate the suitable kinetic models of the process. The FT-IR of AWPGC before adsorption revealed the functional group as hydroxyl, alkanes, carbonyl group, ether and amine group, while after adsorption showed the presence of hydroxyl, aromatic hydrocarbon and silicone. The adsorption kinetic models for both CPF and DDVP fitted most to the pseudo-second-order model, while their best-fitted mass transfer model is Weber Morris.*

Keywords *- Adsorption, Chlorpyrifos, Dichlorvos, Poly-sorbent, Waste Plastic Products.*

1. Introduction

Agriculture holds significant importance for many economies worldwide; however, produce like fruits and crops face threats from pest infestation and diseases. The utilization of pesticides is widely acknowledged as an effective method to mitigate the impact of these challenges on agricultural output. Pesticides play a crucial role in enhancing crop yields and safeguarding crops against pests. Nonetheless, the extensive application and disposal of pesticides for pest control have led to the release of their residues into natural water sources, thereby creating an environmental concern. [1]

Agrochemical products [2, 3] have been detected in both surface and ground waters, constituting a significant concern. Agricultural activities have been pinpointed as the principal origin of agrochemicals found in surface and ground waters [2]. The surge in global population has spurred a corresponding rise in the consumption of plastics and plastic goods. The unregulated disposal of plastic waste poses a significant threat to the environment, manifesting in various detrimental forms such as degradation of natural landscapes, entrapment and mortality of marine life, and obstruction of urban sewage systems, particularly prevalent in emerging economies. These practices foster conditions conducive to the proliferation of disease vectors like mosquitoes, alongside emitting unpleasant odors and impeding water infiltration and soil aeration in agricultural zones, thereby hampering land productivity [4].

Numerous agrochemicals, predominantly pesticides, are frequently identified in Wastewater Treatment Plants (WWTPs), serving as significant sources of pollution [4]. Among these pesticides, Chlorpyrifos (CPF) and Dichlorvos (DDVP) are of particular concern due to their widespread use in agricultural practices for insect, pest, and weed eradication [5].

CPF is frequently utilized as a substitute for toxic pesticides in agriculture due to its lower toxicity compared to other organophosphates. Exposure to CPF and its metabolites poses risks to humans, leading to various nerve disorders, as documented by [6]. Symptoms of acute poisoning from CPF include nausea, headache, convulsions, muscle twitching, and potentially fatal outcomes. Additionally, certain human birth defects have been linked to CPF and its derivatives. On the other hand, DDVP, also known as 2,2-dichlorovinyl-O, O-dimethyl phosphate, is commonly employed to control insects and pests in vegetable and agricultural production, as stated by [7]. DDVP finds extensive use in pest eradication in agriculture, particularly in tomato cultivation, owing to its cost-effectiveness and broad-spectrum bioactivity [8].

Anthropogenic activities and industrial outputs contribute to an escalating presence of emerging contaminants in the natural environment [1, 25]. The anthropogenic activities have been extensively studied worldwide, and no definitive solutions have been proposed for the issue of emerging contaminants, notably pharmaceuticals (including hormones, antibiotics, and others), cosmetics, synthetic dyes, and pesticides, which pose significant concerns in numerous global regions [8,26]. The global production of micro-contaminants has now reached approximately 500 million tons per year [8,27]. There are certain pesticides, due to their stability over time, can be transported through water and air, contaminating areas far from their original sources [7,28]. The sporadic use of pesticides has adversely affected ecosystems, posing threats to birds, wildlife, domestic animals, fish, and livestock [28].

Numerous wastewater treatment methods are available for removing pesticides from industrial effluents, encompassing a combination of physical, chemical, and biological techniques, as highlighted by [7]. These methods, including membrane separation, solvent extraction, steam stripping, hot gases, ion exchange, photodecomposition, and adsorption, are extensively discussed in the literature [8,9,10,11]. However, each of these treatment techniques presents its own merits and limitations, particularly concerning capital and operational costs, efficiency, operability, reliability, environmental impact, pre-treatment requirements, and the generation of sludge and toxic byproducts, as noted by [12]. Many of these technologies prove to be prohibitively expensive to operate, especially when applied to the treatment of large streams.

Adsorption stands out as one of the efficient techniques utilized in the treatment of industrial effluents, given its widespread application owing to its cost-effectiveness in design, operating costs, and high efficiency compared to alternative processes [13,14,15,16]. The use of various adsorbents in the remediation of wastewater polluted with pesticides such as CPF and DDVP has been reported by many researchers. However, a report on the use of WPGC composite for the remediation of wastewater containing a mixture of CPF and DDVP has not been seen so far. This research work focused on maximizing the synergetic effect of the mixture of waste plastic products as an adsorbent for the remediation of some organophosphate pesticides, such as CPF and DDVP, from wastewater. This, therefore, shows the research gap and originality of the focus of this study.

2. Materials and Methods

2.1. Materials, Reagents and Equipment

The basic materials used in this experiment were Waste Plastic Chair Granules (WPCG), Waste Polyvinyl Chloride (WPVC), Waste Jerry Can Granules (WJCG) and Waste Electronic Casing Grains (WECG). The materials were sourced from the plastic collection center at Eiyekorin, Ilorin (8° 30′N / 4° 32′ E), Kwara State, Nigeria. The reagents used in this study included Methanol (0.1 M CH_3OH, molecular weight; 32.04 g/mol), Acetic acid (0.3 M CH_3COOH, molecular weight; 60.05 g/mol), Sodium Hydroxide (NaOH), Chlorpyrifos ($C_9H_{11}Cl_3NO_3PS$, molecular weight; 350.59 g/mol, ultraviolet (UV) absorbance value; 290 nm) and Dichlorvos, also called DDVP ($C_4H_7Cl_2O_4P$, molecular weight; 220.98 g/mol, ultraviolet (UV) absorbance value: 239 nm).

2.2. Methods

2.2.1. Adsorbent Preparation

The Raw materials (WPCG, WPVC, WJCG and WECG) were sourced from the waste plastic collection center at Eiyekorin (8°30′N / 4°32′ E), Kwara State, Nigeria and moved to the Bioenvironmental Water and Engineering Research Group (BWERG) Laboratory, LAUTECH, Ogbomoso. Stones and other debris were removed from the plastic samples after collection. The plastic samples were washed, dried and milled to 840 µm [17].

2.2.2. Pre-treatment and Activation of Plastic Samples

Each plastic sample was pretreated with 0.1 M methanol solution (40: 100 g:100 mL) to remove any other surface contaminant and then dried to constant weight [17,18]. The sample was acetylated with 0.3 M acetic acid at room temperature to obtain Activated Waste Plastic Chair Granules (AWPCGs) (Khorram *et al.,* 2017; Ali *et al.,* 2019). The AWPCGs were kept in an airtight container labeled for subsequent use (Djahed *et al.,* 2016). The same procedure was repeated for WPVC, WJCG and WECG to obtain AWPVCGs, AWJCGs and AWECGs, respectively. The optimization of the composite composition under Simplex Lattice Design (SLD) of the Mixture Methodology (MM) of the Design Expert (DOE 12.0.1) was used in a preliminary study [19].

2.3. Fourier Transform Infrared Spectroscopy Characterisation of Adsorbents

The analysis of Fourier Transform Infrared Spectroscopy (FT-IR) aimed to discern alterations in the functional groups of both raw and activated samples. Tablets containing each

sample mixed with potassium bromide (at a 1:100 ratio) were prepared for analysis. The FT-IR spectra were recorded within the frequency range of 4000 cm-1 to 400 cm-1 using a SHIMADZU FTIR-8400S spectrometer, with a detector at 4 cm-1 resolution and 200 scans per sample. The FTIR spectrum's peak values identified the functional groups of the active components, with the separation based on their peak ratio [19]. The attenuated total reflection, measured as a function of wavelength, produced an adsorption spectrum of the adsorption medium, following the principle of Fourier Transform Infrared Spectroscopy [20].

2.4. Batch Adsorption Study

The adsorption characteristics of the developed WPGC were evaluated through batch studies aiming at the removal of CPF and DDVP from aqueous media. One gram (1 g) of the WPGC was introduced into a 100 mL aqueous solution containing CPF and DDVP at a concentration of 100 mg/l and a pH of 7 ± 0.1 [21]. Contact time effects were investigated by subjecting the mixture to batch adsorption at mixed ratios of 1:1 on the WPGC, with agitation at 150 rpm in a rotary shaker for durations ranging from 10 to 225 minutes at room temperature. The resulting solution containing pesticides that were not adsorbed underwent decantation then, followed by centrifugation at 1000 rpm for 5 minutes [16]. Analysis of the supernatant was performed using a UV-VIS spectrophotometer (Model UV752 (D)) at wavelengths of 239 nm for Chlorpyrifos and 290 nm for DDVP to quantify the remaining amounts of each pesticide in the solution.

2.5. Adsorption Kinetic Studies

Various adsorption kinetic models (Equation 1-6) and mass transfer diffusion models (Equation 7-9) were selected for this study (Table 1) to determine which of them was most suitable to describe the mass transfer mechanism that occurred in the adsorption of CPF and DDVP were evaluated to determine the most suitable model to describe the adsorption of CPF and DDVP.

3. Results and Discussion

3.1. Fourier Transform Infrared Characteristics of the Developed WPGC

Figure 1a displays the FTIR spectra of the WPGC before adsorption, revealing the presence of broad absorption peaks (Table 1). The peak observed at 3775.10 cm-1 indicates the presence of hydroxyl groups (OH), responsible for binding onto the adsorbent, with a transmittance of 85.70%. At 3350.19 cm-1, the peak signifies stretching vibrations of alkane groups and aliphatic acids, with a transmittance of 39.56%. Similarly, the peak at 2775.84 cm-1 suggests the presence of carbonyl groups (C-O-C) with a transmittance value of 62.48%. Additionally, at 1250.78 cm-1, a peak with a transmittance of 43.16% indicates the presence of hydroxyl, ester, and ether (C-O) functional groups on the adsorbent's surface [22]. Finally, the peak at 1150.13 cm-1, with a transmittance of 63.76%, demonstrates the stretching variation of ether (C-O-C).

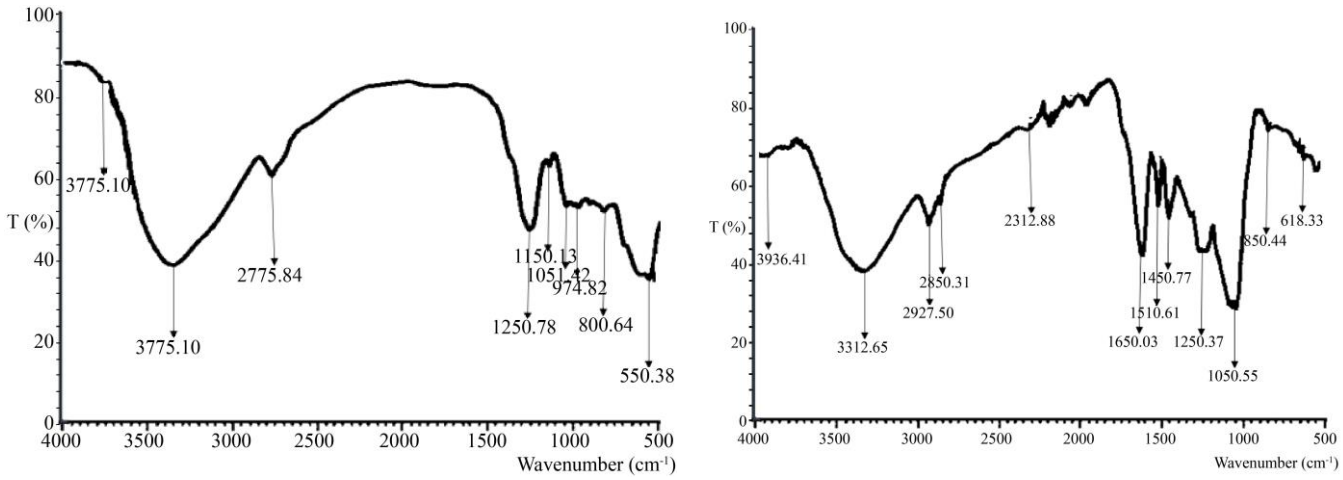

Fig. 1 FTIR of WPGC (a) before adsorption and (b) after adsorption

The peak value at 1051.42 cm^{-1} indicates Amine group C-N is responsible for stretching vibration (Cyanide ion) with a transmittance value being 52.18%. The peak value of 974.82 cm^{-1} indicates the presence of Glycoside α-glycosidic linkage responsible for stretching vibration. The peak value at 800.64 cm^{-1} indicates the presence of a phosphate group (P-O-C) responsible for stretching vibration. In Run 9, the peak value was 550.38 $cm^{-1,}$ indicating the presence of aliphatic organohalogen compounds C-Br stretching vibration; the transmittance was 37.83 %.

Table 1. Waste Plastic Granule Composite before and after adsorption

Peak Wavelength cm^{-1}	Before Adsorption			Peak Wavelength cm^{-1}	After Adsorption		
	Transmittance (%)	Bond Type	Functional Group		Transmittance (%)	Bond Type	Functional Group
3775.10	85.70	O-H	Hydroxyl group	3926.41	69.52	O-H	Hydroxyl
3350.19	39.56	C-H	Alkanes	3312.65	39.36	C-O	Carboxylic group
2775.84	62.48	C-O-C	Carbonyl group	2927.50	48.95	CH_3	Alkanes
1250.78	43.16	C–O	Hydroxyl, Ester and Ether	2850.31	56.08	C-H	Alkanes
1150.13	63.76	C-O-C	Ether	2312.88	72.24	N-H	Amino acid, amino-related
1051.42	52.18	C-N	Amine group	1650.03	43.26	C-H	Alkanes
974.82	52.26	α-glycosidic linkage	Glycoside	1510.61	56.04	C=C	Aromatic hydrocarbon groups
800.64	52.25	P-O-C	Phosphate group	1450.77	54.98	C-H	Secondary alcohol

The spectra of the FTIR of the WPGC after adsorption, shown in Figure 1b, indicate the presence of broad adsorption peaks at 3926.41 cm^{-1} as indicated in Table 2, the presence of the Hydroxyl group OH group was responsible for the O–H stretching vibration of hydroxyl and phenolic group and transmittance was at 69.52 %. The peak 3312.65 cm^{-1} indicates Alkanes group C-H -CH asymmetric stretching vibration, and the transmittance was 39.36 %. The peak value of 22927.50 cm^{-1} indicated the presence of Lipid group CH_3 asymmetry stretching vibration with a transmittance value of 48.95%. In comparison, the peak value at 2850.31 cm^{-1} indicates the presence of C-H stretching vibration, and the transmittance value was 56.08 % [22].

The peak value at 2312.88cm^{-1} shows the presence of Amino acid and amino-related N-H stretching vibrations; the transmittance value was 72.24%, while at 1650.03 cm^{-1} indicates Carbonyls and carboxylic, with a transmittance value being 43.26%. The peak value at 1510.61 cm^{-1} indicates the presence of Aromatic hydrocarbon groups and Stretching vibration of C=C groups due to the aromatic ring. In contrast, 1450.77 cm^{-1} indicates the presence of secondary alcohol responsible for deformation vibration.

The peak value was 1250.57 $cm^{-1,}$ indicating the presence of Ether group C-O stretching vibration of ether and alcohol, and the transmittance was 43.79%. The peak values at 1050.55 cm^{-1} and 850.44 cm^{-1} indicated the presence of Alkane C-H, which was responsible for skeletal vibration [22]. The peak value at 618.331 cm^{-1} shows the presence of organic siloxane or silicone responsible for Si–O–Si stretching vibration.

3.2. Kinetic Studies for the Adsorption of CPF and DDVP

The study of kinetic data underwent processing to comprehend the dynamics of the adsorption reaction, focusing on the order of the rate of reaction. Various models, including zero order, pseudo-first order, pseudo–second–order, Elovich, Avram and Fractional power models, were employed. The fit of these models was assessed through their corresponding linear plots to derive parameters and compare the Regression R^2 of each expression for optimal fit.

3.2.1. Zeroth Order Kinetic Model

The plot of q_t against t (Figure 2a) was used to evaluate the zeroth order kinetic (Equation 1), such as K_o, q_o, and R^2. K_o was found to be 0.0014 for CPF while for DDVP, it was 0.0005, where q_o for CPF was 0.6165 and for DDVP it was 0.0953. R^2 values for DDVP were found to be greater than that of CPF 0.9172 > 0.7692. The R^2 values for this study were not far from unity, and this can be used to fit the adsorption of CPF and DDVP in WPGC.

$$q_t = q_O + K_o t \quad (1)$$

3.2.2. Pseudo-First-Order Kinetic Model

The estimated first-order (Equation 2) equilibrium rate constant K_1 and q_1 were evaluated from the plot of ln ($q_e - q_t$) against t (Figure 2b). The values of q_1 were in the range of 0.013 and 0.0068 for CPF and DDVP, respectively; q_1 for CPF was found to be 0.3006, and DDVP was 0.1454. The R^2 obtained for CPF was 0.9648 as against that of DDVP of 0.9664. The result indicates the adsorption of CPF and DDVP was consistent with a pseudo-first-order kinetic Equation, and the adsorption was maintained via chemisorption.

$$\ln(q_e - q_t) = \ln q_e - k_1 t \quad (2)$$

3.2.3. Pseudo-Second-Order Kinetic Model

The pseudo-second-order model (Equation 3) was used to assess the various values of K_2 and q_2. The evaluation was performed through the plot of t/q_t against t, as depicted in Figure 2c. In this context, K_2 for DDVP was observed to be higher than that of CPF, while the q_2 for CPF (0.8734) outperformed that of DDVP (0.2091). The obtained R_2 value for CPF, which was 0.9993, surpassed the values for DDVP and closely matched the qe experimental values. This result indicated that CPF exhibited a better fit than the pseudo-first-order kinetics model. A comparison between the experimental and calculated values for qe revealed that the pseudo-second-order adsorption kinetics model yielded larger calculated values. In contrast, the pseudo-first-order model produced smaller calculated values. The calculated values of the pseudo-second-order model were found to be closer to the experimental values, suggesting its superiority over the pseudo-first-order model. Specifically, the R^2 for CPF in the pseudo-second-order model was 0.9993, outperforming the R_2 for the pseudo-first-order model (0.9648). For DDVP, the R^2 values in the pseudo-second-order and pseudo-first-order models were 0.9872 and 0.9664, respectively, confirming the superiority of the pseudo-second-order model over the pseudo-first-order model, as reported by Sahoo *et al.* in 2018.

$$t/q_t = \frac{1}{K_2 q_e^2} + t/q_e \quad (3)$$

3.2.4. Elovich Kinetic Model

The evaluation was conducted using the plot of q_t against t (Equation 4). Notably, the parameter Ke for CPF (9.5512) was observed to be less than that of DDVP (27.008), while the q_e for CPF (1.939 mg/L) was greater than that of DDVP (0.030 mg/L). The R_2 values for CPF and DDVP in the Elovich model were 0.9792 and 0.9239, respectively. The linear relationship between q_t and t in the graph, as depicted in Figure 2d, indicated a good fit. However, despite the reasonably high R_2 values, it was concluded that the pseudo-second-order model (PSO) provided a better fit than the Elovich model for the adsorption of CPF and DDVP in WPGC, supported by the superior R_2 in the PSO model.

$$q_t = \frac{\ln q_e K_e}{K_e} + \frac{1}{K_e}\ln t \quad (4)$$

3.2.5. Fractional Power Kinetic Model

The plot of log q_t against log t, as stated in Equation 5, is shown in (Figure 2e) provides a linear relationship from which v and k are determined from the slope, and the intercept of the plot K_{fp} for CPF was 0.3905 while that of DDVP was 0.04543. The value of V in DDVP, which was 0.2693, was higher than that of CPF (0.1519). The values of V being positive and less than unity coupled with the closeness of R^2 (0.9628 for CPF and 0.9239 for DDVP) to unity indicates a good fitting of the kinetic data to the fractional power model.

$$Log\ q_t = log\ K + v log\ t \quad (5)$$

3.2.6. Avrami Kinetic Model

The plot of ln ($q_e/(q_e-C_e)$) against ln t, in this case, a linear relationship was obtained from which n_{av} and k_{av} were detained from the slope and intercept of the plot (Figure 2f). The n_{av} values increased from 0.4341 for CPF to 0.4456 for DDVP (Table 2). The value of R^2 for CPF and DDVP were 0.9865 and 0.9271, respectively. A similar result was obtained by [23].

$$\mathrm{In}\left[ln\left(\frac{q_m}{q_m - q_t}\right)\right] = n_{av} ln K_{av} + n_{av} lnt \quad (6)$$

3.3. Effectiveness of Adsorption Kinetic Model

The validation of kinetic models was determined using R^2 to unity coupled with good agreement between the experimental and the calculated quantity adsorbed. The better kinetic model in observing the data. Based on the evaluated parameters. The results revealed that kinetic models fitted best with Pseudo second order, and the least was at Zero order kinetic based on the highest value of R^2 as shown in Table 2. This means that the pseudo-second-order model better describes the adsorption process; meanwhile, K_2 obtained is closer to the values obtained from experimental data, which is in agreement with the result obtained by [24].

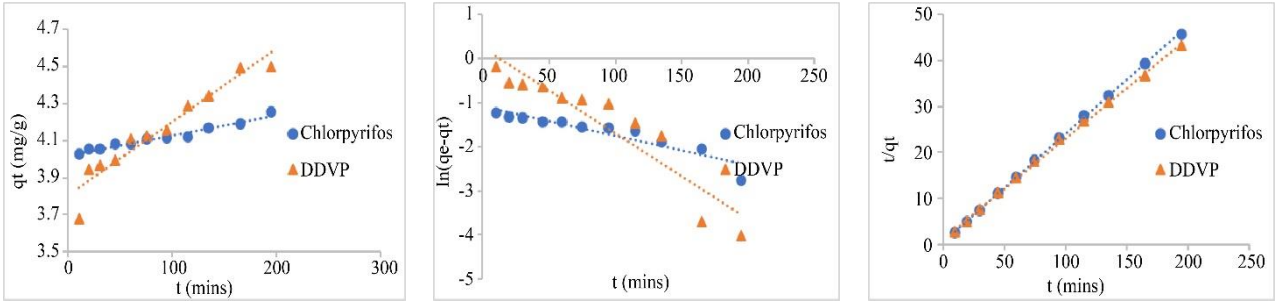

(a) **(b)** **(c)**

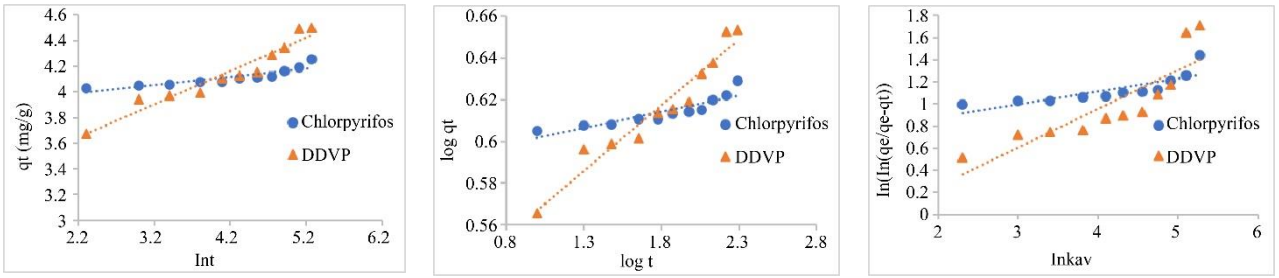

(d) **(e)** **(f)**

Fig. 2 (a) Zeroth Order Kinetic, (b) Pseudo First Order Model, (c) Pseudo Second Order Model, (d) Elovich Kinetic Model, (e) Functional Power Model and (f) Avrami Kinetic Model

Table 2. Adsorption Kinetic Studies of Chlorpyrifos and Dichlorvos

Kinetics	Parameter	CPF	DDVP
Zero order kinetic	k_o	0.0014	0 0.0005
	q_o	0.6165	0.0953
	R^2	0.7692	0.9172
Pseudo First-Order Model (PFO)	k_1	0.013	0.0068
	q_1	0.3006	0.1454
	R^2	0.9648	0.9664
Pseudo Second Order Model (PSO)	k_2	0.1254	0.1775
	q_2	0.8734	0.2091
	R^2	0.9993	0.9872
Elovich Model	k_e	9.551	27.701
	q_e	1.939	0.030
	R^2	0.9792	0.9239
Functional Power Model	k_{fp}	0.3905	0.04543
	V	0.1519	0.2693
	R^2	0.9628	0.9373
Avrami Model	k_{av}	0.08188	0.01471
	n_{av}	0.4341	0.4458
	R^2	0.9865	0.9271

K (min^{-1}) is the rate constant, and q_e (mg/g) is the adsorbed quantity at equilibrium.

3.4. Mass Transfer Models

Mass transfer models such as Webber-Morris, McKay and Mathew-Weber diffusion models were used to study the mass transfer diffusion in this study.

3.4.1. Weber-Morris Diffusion Model

The intra-particle diffusion constants K_{wm} ($mg/g^{0.5}$) and A (mg/g) were obtained from the plot of q_t against $t^{0.5}$ shown in Figure 3 as stated in Equation 7. The constant values K_{wm} and A are obtained from the plot, and R^2 was also estimated from the plot as shown in Table 3; the values of K_{wm} obtained were 0.0184 and 0.0699 $mg/g^{0.5}$ for CPF and DDVP, respectively, which indicates that several stages of adsorption took place. The values for A stand for the significance of the boundary layer effect on the thickness of the adsorption study; the value was found to be 3.9551 and 3.5429 mg/g for CPF and DDVP, respectively. The intraparticle diffusion constant is also found to be directly proportional to the boundary layer thickness (A). The value of R^2 decreased from 0.9575 to 0.9115, as shown in Table 3. The plot, as indicated in Figure 3a, did not pass through the origin, and the intraparticle diffusion is not sufficient to determine the sole rate-limiting step.

$$q_t = K_{WM}\sqrt{t} + A \quad (7)$$

3.4.2. Dumwald -Wagner Diffusion Model

The plot of log $(1\text{-}F)^2$ against t, as shown in Figure 3b, gives insight into the significance of the Dumwald Wagner diffusion mode (Equation 8). The values of the interparticle diffusion parameter K_{DW} were obtained from the plot and R^2 was also determined from the plot; there is no intercept. The values of K_{DW} obtained for CPF and DDVP were -0.0216 and -0.0242 and their corresponding R^2 are 0.8155 and 0.9506, respectively. This model is not fit due to the low values of R^2 compared with the Weber–Morris diffusion model above.

$$In\frac{C}{C_o} = -K_{MW}At \quad (8)$$

3.4.3. Mathew-Weber McKay Film Transfer Diffusion

The slope of the graph, in the graph of ln (1-F) against time (t), indicates intra-particle diffusion constant K_m (Figure 3c). The values of K_m and R^2 were estimated from the plot as shown in Table 3; the values of Km obtained from the plot were 0.0270 and 0.0296 for CPF and DDVP, while their corresponding coefficients of correlation were 0.7926 and 0.9312, respectively.

This model did not show a good fit for the experimental data. It shows the adsorption mechanism. In this case, adsorbate is transported from the bulk solution to the external surface of the adsorbent. The values of R^2 were low compared with the Weber-Morris diffusion model. The values of R^2 for CPF and DDVP for Weber-Morris diffusion are close to unity; therefore, the Weber-Morris diffusion model fits best

$$Log\ (1 - F^2) = -\frac{K_{DW}}{2.303}t \quad (9)$$

But $F = \frac{q_t}{q_e}$

The parameters of Equations 1-9 are defined as follows: q_o is the amount of solute sorbed at time t = 0 (mgg^{-1}), qt (mgg^{-1}) is the amount of solute sorbed on the surface of the sorbent at any time, t, and K_o is the zero-order reaction rate constant, (mg/g min), q_e is the adsorption capacity at equilibrium (mg/g), k_1 is the pseudo-first-order rate constant (l/min), k_2 (mg/g/min), is the pseudo-second-order rate constant K_e is Elovich constant (g/mg). K and v are the Fractional Power model constants, k_{av} and n_{av} are the Avrami adsorption kinetics constants. A(mg/g) is a parameter that indicates the interfacial film resistance or boundary layer effect. In contrast, K_{wm} ($mg/gmin^{-0.5}$) is the intraparticle diffusion rate constant, F is the adsorption capacity ratio concerning time and equilibrium, and K_{DW} is the Dumwald-Wagner diffusion rate constant.

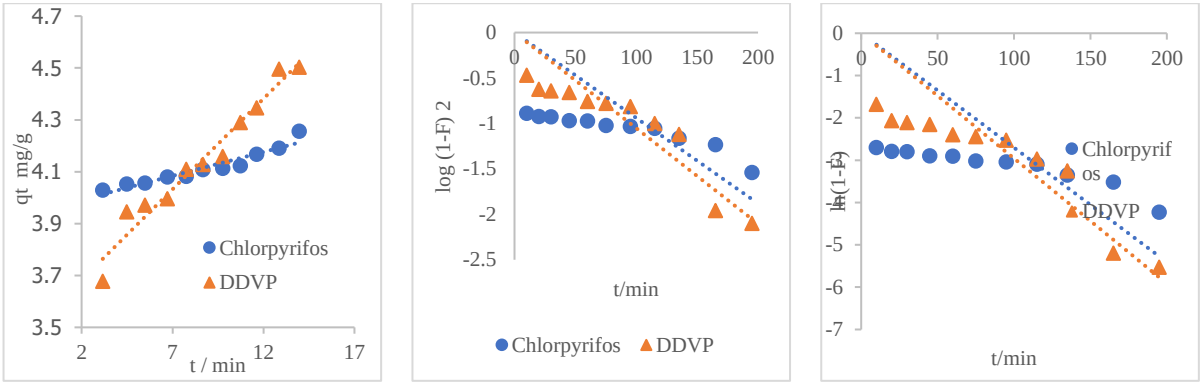

(a) **(b)** **(c)**

Fig. 3 (a) Weber Morris Mass Transfer Diffusion Mode, (b) Dumwald Wagner Mass Transfer Mode and (c) McKay Film Mass Transfer Mode

Table 3. Mass transfer models

Mass Transfer Models	Parameter	CPF	DDVP
Weber Morris	K_{WM}	0.0184	0.0699
	A	3.9551	3.5429
	R^2	0.9115	0.9575
Dumwald Wagner	K_{DW}	-0.0216	-0.0242
	R^2	0.8155	0.9506
McKay Film	K_M	0.0270	0.0296
	R^2	0.7926	0.9312

K_{WM} (mg/g min $^{0.5}$) A(mg/g), K_{DW} and K_M are dimensionless quantities.

4. Conclusion

The possibility of producing chemically effective adsorbent from quaternary mixtures of waste plastic products for the remediation of wastewater containing CPF and DDVP pesticide mixtures was studied. The following conclusions were made based on the analysis of the results obtained. The adsorbent developed from the selected waste plastic products (WPGC) proved to be an effective material for the remediation of wastewater containing CPF and DDVP. The FTIR of WPGC before adsorption showed the functional group of the adsorbent as hydroxyl, alkanes, carbonyl group, ether and amine group, while after adsorption showed the presence of hydroxyl, Lipid, aromatic hydrocarbon and silicone. The adsorption kinetic models for both CPF and DDVP fitted most to the pseudo-second-order model, while their best-fitted mass transfer model is Weber Morris**.**

Acknowledgments

Members of the Bioenvironmental Water and Engineering Research Group (BWERG) Laboratory, LAUTECH, Ogbomoso, appreciate the opportunity given to me to make use of the Research Laboratory for experiments and analyses.

References

[1] K. Sosnowska-Nosek, K.Styszko-Grochowiak, and J. Gołas, "Emerging Contaminants in Aquatic Environment-Sources, Risk and Analytical Problems," *Environmental Technology*, vol.24, pp. 44-48, 2014.

[2] José Augusto Monteiro de Castro Lima et al., "Modern Agriculture" Transfers many Pesticides to Watercourses: A Case Study of a Representative Rural Catchment of Southern Brazi," *Environmental Science and Pollution Resources*, vol. 27, pp. 10581-10598, 2020. [CrossRef] [Google Scholar] [Publisher Link]

[3] Luca Carena, Silvia Comis, and Davide Vione, "Geographical and Temporal Assessment of the Photochemical Decontamination Potential of River Waters from Agrochemicals: A first Application to the Piedmont Region (NW-Italy)," *Chemosphere*, vol. 263, 2021. [CrossRef] [Google Scholar] [Publisher Link]

[4] Lei Tang et al., "Removal of Trace Organic Pollutants (Pharmaceuticals and Pesticides) and Reduction of Biological Effects from Secondary Effluent by Typical Granular Activated Carbon," *Science of The Total Environment*, vol. 749, 2020. [CrossRef] [Google Scholar] [Publisher Link]

[5] Marie E. DeLorenzo, Geoffrey I. Scott, and Philippe E. Ross, "Toxicity of Pesticides to Aquatic Microorganisms: A Review," *Environmental Toxicology, Chemical Engineering*, vol. 20, no. 1, pp. 84-98, 2018. [CrossRef] [Google Scholar] [Publisher Link]

[6] R. McKinlay et al., "Endocrine Disrupting Pesticides: Implications for Risk Assessment," *Environmental Toxicology*, vol. 34, no. 2, pp. 168-183, 2018. [CrossRef] [Google Scholar] [Publisher Link]

[7] Xiaobin Yu et al., "Synergistic Effects of the Combined Use of Ozone and Sodium Percarbonate for the Oxidative Degradation of Dichlorvos," *Journal of Water Processing Engineering*, vol. 39, 2021. [CrossRef] [Google Scholar] [Publisher Link]

[8] Yuming Zhang et al., "Emerging Technologies for Degradation of Dichlorvos: A Review," *International Journal of Environmental Resources in Public Health*, vol. 18, no. 11, pp.1-23, 2021.[CrossRef] [Google Scholar] [Publisher Link]

[9] Mohammad Boshir Ahmed et al., "Progress in the Biological and Chemical Treatment Technologies for Emerging Contaminant Removal from Wastewater A Critical Review," *Journal of Hazardous Materials*, vol. 323, pp. 274-298, 2017. [CrossRef] [Google Scholar] [Publisher Link]

[10] Kiran Meghwal et al., "Chemical and Biological Treatment of Dyes," *Impact of Textile Dyes on Public Health and the Environment*, pp. 170-204, 2019. [CrossRef] [Google Scholar] [Publisher Link]

[11] Qiongfang Wang et al., "Impact of Zero-Valent Iron/Persulfate Peroxidation on Disinfection Byproducts through Chlorination of Alachlor," *Chemical Engineering Journal*, vol. 380, 2020. [CrossRef] [Google Scholar] [Publisher Link]

[12] Adolfo Marican, and Esteban F. Durán-Lara, "A Review on Pesticide Removal through Different Processes" *Environmental Science Pollution and Resources*, vol. 25, pp. 2051-2064, 2018. [CrossRef] [Google Scholar] [Publisher Link]

[13] Sebastian R. Sørensen, Christian N. Albers, and Jens Aamand, "Rapid Mineralization of the Phenylurea Herbicide Diuron by Variovorax Sp. Strain SRS16 in Pure Culture and within a Two-Member Consortium," *Environmental of Microbiology*, vol. 74, no. 8, pp. 2332-2340, 2018. [CrossRef] [Google Scholar] [Publisher Link]

[14] Himanshu Patel, "Fixed-Bed Column Adsorption Study: A Comprehensive Review" *Applied Water Science*, vol. 9, no.3, 2019. [CrossRef] [Google Scholar] [Publisher Link]

[15] M.O. Aremu et al., "Improved Phenol Sequestration from Aqueous Solution using Silver Nanoparticle-Modified Palm Kernel Shell Activated Carbon" *Heliyon*, vol. 6, no. 7, 2020. [CrossRef] [Google Scholar] [Publisher Link]

[16] Idris Olanrewaju Okeowo et al., "Adsorption of Phenol from Wastewater using Microwave-Assisted Ag-Au Nanoparticle-Modified Mango Seed Shell Activated Carbon," *International Journal of Environmental Research*, vol. 14, pp. 215-233, 2020. [CrossRef] [Google Scholar] [Publisher Link]

[17] Imran Ali et al., "Grachev, Graphene-based Adsorbents for Remediation of Noxious Pollutants from Wastewater," *Journal of Environmental Engineering*, vol. 127, pp.160-180, 2019. [CrossRef] [Google Scholar] [Publisher Link]

[18] Mohammad Khorram, Ahmad Mousavi, and Nasir Mehranbod, "Chromium Removal using Adsorptive Membranes Composed of Electrospun Plasma Treated Functionalized Polyethylene, Terephthalate with Chitosan," *Journal of Environmental Chemical Engineering*, vol.5 no. 3, pp. 2366-2377, 2017. [CrossRef] [Google Scholar] [Publisher Link]

[19] Mahsa Najafi Lahiji, Ali Reza Keshtkar, and Mohammad Ali Moosavian, "Adsorption of Cerium and Lanthanum from Aqueous Solutions by Chitosan/Polyvinyl Alcohol/3-Mercaptopropyltrimethoxysilane Beads in Batch and Fixed-Bed Systems," *Particulate Science Technology*, vol. 36, no. 3, pp. 340-350, 2018. [CrossRef] [Google Scholar] [Publisher Link]

[20] Adel Fisli et al., "Isotherm, Kinetic and Thermodynamic Adsorption Studies of Dye Waste Paper Activated Carbon," *Journal Technology of Science and Engineering*, vol. 83, no. 1, pp. 45-55, 2021. [Google Scholar]

[21] Nuria Vela et al., "Reclamation of Agro-Wastewater Polluted with Pesticide Residues using Sunlight Activated Persulfate for Agricultural Reuse," *Science and Total Environment*, vol. 660, pp. 923-925, 2019. [CrossRef] [Google Scholar] [Publisher Link]

[22] Hala M. Hamadeen et al., "Novel Low-Cost Nanoparticles for Enhanced Removal of Chlorpyrifos from Wastewater: Sorption kinetics, and Mechanistic Studies," *Arabian Journal of Chemical Engineering*, vol. 14, no. 3, 2021. [CrossRef] [Google Scholar] [Publisher Link]

[23] M. Benallou Benzekr et al., "Valorization of Olive Stones into a Granular Activated Carbon for the Removal of Methylene Blue in Batch and Fixed Bed Mode," *Journal of Material and Environmental Science*, vol. 9, no. 1, pp. 272-284, 2018. [Google Scholar] [Publisher Link]

[24] Aderonke A. Okoya et al., "Comparative Assessment of the Efficiency of Rice Husk Biochar and Conventional Water Treatment Method to Remove Chlorpyrifos from Pesticide Polluted Water," *Current Journal of Applied Science and Technology*, vol. 39, no. 2, pp. 1-11, 2020. [CrossRef] [Google Scholar] [Publisher Link]

[25] Ngozi H. Arihilam, and E.C. Arihilam, "Impact and Control of Anthropogenic Pollution on the Ecosystem- A Review," *Journal of Bioscience and Biotechnology*, vol. 4, no. 3, pp. 54-59, 2019. [CrossRef] [Google Scholar] [Publisher Link]

[26] Inês B. Gomes, Lúcia C. Simões, and Manuel Simões, "The Effects of Emerging Environmental Contaminants on Stenotrophomonas Maltophilia Isolated from Drinking Water in Planktonic and Sessile States," *Science and Total Environment*, vol. 643, pp. 1348-1356, 2018. [CrossRef] [Google Scholar] [Publisher Link]

[27] N. Thomaidis, A. Asimakopoulos, and A. Bletsou, "Emerging Contaminants: A Tutorial Mini-Review," *Water Engineering*, vol. 14, pp. 4-20, 2012. [CrossRef] [Google Scholar] [Publisher Link]

[28] Giusy Lofrano et al., "Occurrence and Potential Risks of Emerging Contaminants in Water," *Visible Light Active Structured Photocatalysts for the Removal of Emerging Contaminants*, pp. 1-25, 2020. [CrossRef] [Google Scholar] [Publisher Link]